

# Radiobiological Effectiveness of Ultrashort Laser-Driven Electron Bunches: Micronucleus Frequency, Telomere Shortening and Cell Viability

Maria Grazia Andreassi,<sup>a,1</sup> Andrea Borghini,<sup>a</sup> Silvia Pulignani,<sup>a</sup> Federica Baffigi,<sup>b</sup> Lorenzo Fulgentini,<sup>b</sup> Petra Koester,<sup>b</sup> Monica Cresci,<sup>a</sup> Cecilia Vecoli,<sup>a</sup> Debora Lamia,<sup>c</sup> Giorgio Russo,<sup>c</sup> Daniele Panetta,<sup>a</sup> Maria Tripodi,<sup>a</sup> Leonida A. Gizzi<sup>b</sup> and Luca Labate<sup>b</sup>

<sup>a</sup> Genetics Unit, CNR Institute of Clinical Physiology, Pisa, Italy; <sup>b</sup> Intense Laser Irradiation Laboratory, CNR National Institute of Optics, Pisa, Italy; and <sup>c</sup> CNR Institute of Bioimaging and Molecular Physiology, Cefalù (PA), Italy

---

Andreassi, M. G., Borghini, A., Pulignani, S., Baffigi, F., Fulgentini, L., Koester, P., Cresci, M., Vecoli, C., Lamia, D., Russo, G., Panetta, D., Tripodi, M., Gizzi, L. A. and Labate, L. Radiobiological Effectiveness of Ultrashort Laser-Driven Electron Bunches: Micronucleus Frequency, Telomere Shortening and Cell Viability. *Radiat. Res.* 186, 245–253 (2016).

Laser-driven electron accelerators are capable of producing high-energy electron bunches in shorter distances than conventional radiofrequency accelerators. To date, our knowledge of the radiobiological effects in cells exposed to electrons using a laser-plasma accelerator is still very limited. In this study, we compared the dose-response curves for micronucleus (MN) frequency and telomere length in peripheral blood lymphocytes exposed to laser-driven electron pulse and X-ray radiations. Additionally, we evaluated the effects on cell survival of *in vitro* tumor cells after exposure to laser-driven electron pulse compared to electron beams produced by a conventional radiofrequency accelerator used for intraoperative radiation therapy. Blood samples from two different donors were exposed to six radiation doses ranging from 0 to 2 Gy. Relative biological effectiveness (RBE) for micronucleus induction was calculated from the alpha coefficients for electrons compared to X rays ( $RBE = \alpha_{\text{laser}}/\alpha_{\text{X rays}}$ ). Cell viability was monitored in the OVCAR-3 ovarian cancer cell line using trypan blue exclusion assay at day 3, 5 and 7 postirradiation (2, 4, 6, 8 and 10 Gy). The RBE values obtained by comparing the alpha values were 1.3 and 1.2 for the two donors. Mean telomere length was also found to be reduced in a significant dose-dependent manner after irradiation with both electrons and X rays in both donors studied. Our findings showed a radiobiological response as mirrored by the induction of micronuclei and shortening of telomere as well as by the reduction of cell survival in blood samples and cancer cells exposed *in vitro* to laser-generated electron bunches. Additional studies are needed to improve preclinical validation of the radiobiological characteristics and efficacy of laser-driven electron accelerators in the future. © 2016 by Radiation Research Society

## INTRODUCTION

The field of electron acceleration driven by ultrashort high-intensity laser pulses has undergone impressive development over the past few years, now enabling fast delivery of doses of medical interest with electron bunches of energy from a few MeV up to a few tens or even hundreds of MeV (*1–10*). The application of laser-driven electron accelerators in radiotherapy is particularly appealing. Indeed, from a practical perspective, such a class of novel “table-top” accelerators have a wealth of advantages over conventional ones, mostly due to their reduced footprint, leading, for instance, to less demanding radio-protection requirements. Furthermore, they would allow hundreds of MeV electron beams to be produced with centimeter size “accelerator stages”. Such high-energy beams, which would penetrate very deep into tissue, may represent great potential for the future of radiotherapy (*4–6*). In particular, the output has already been shown to come very close to that of conventional radiofrequency-driven accelerators used for intraoperative radiation therapy (IORT). However, before translating the usage of laser-driven accelerators into clinical practice, one important issue must be addressed, namely the radiobiological effectiveness (RBE) of such ultrashort bunches relative to electron beams by conventional radiofrequency LINACs. Indeed, laser-generated electron bunches exhibit a bunch duration of the order of the laser-driven pulse, namely of the order of 10 femtosecond (fs) (*11*). Such duration can be safely estimated to remain at the ps level while the beam travels to the cell sample/patient position. Considering that the bunch charge is similar to the corresponding value from a typical LINAC used in radiotherapy, instantaneous dose-rate values of up to six orders of magnitude higher are easily achieved in the case of laser-generated electron bunches. DNA damage mediates many of the lethal effects of radiations to cells. The main types of damage are base damages, single-strand breaks (SSBs), double-strand breaks (DSBs) and cluster damages. These types of damage may be caused by a direct radiation effect when a primary or

---

<sup>1</sup> Address for correspondence: CNR Institute of Clinical Physiology, via Moruzzi 1, 56124 Pisa, Italy; email: mariagrazia.andreassi@ifc.cnr.it.

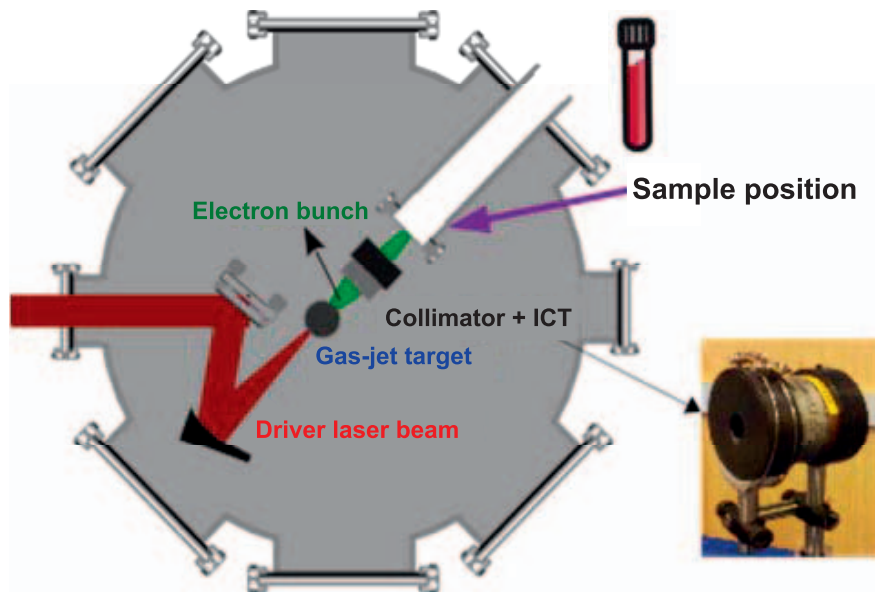


FIG. 1. Schematic layout of the irradiation setup. ICT = integrating current transformer.

secondary radiation particle transfers energy to the DNA molecule, or by an indirect radiation effect as result of water ionization, forming free reactive oxygen species (free radicals), which in turn damage the DNA (12, 13). Considering the duration of a typical laser-generated electron bunch given above and comparing it to the time scale of biological effects of radiation to cells, it may be possible that due to the shortness of the pulses new phenomena of radiation effects arise (12, 13), ultimately resulting in a change of RBE. The micronucleus assay in peripheral blood lymphocytes (PBLs) is a well validated experimental system in radiation biology (14, 15). PBLs are an ideal model for studying the effects of radiation on chromosomal aberrations because they are naturally synchronized in the  $G_0$  phase of the cell cycle and, consequently, all cells have a uniform radiosensitivity (16). Recently, the evaluation of telomere shortening has been suggested as a new biological indicator of radiation exposure (17).

The goal of the current study was to determine the dose-response curve of micronucleus (MN) frequency and telomere length of laser-driven electron pulse and X-ray (reference dose) irradiations for PBLs. Additionally, we evaluated the effects on cell survival after irradiation of *in vitro* tumor cells with laser-driven electron pulses compared to electron beams produced by a conventional radiofrequency accelerator for IORT.

## MATERIALS AND METHODS

### Blood Sampling

Whole blood was collected in both heparin and EDTA vials by venipuncture from two healthy nonsmoking donors (male and female) <30 years of age. A 12 ml blood sample was taken and divided into six sterilized culture bottles with heparin anticoagulant.

To demonstrate reproducibility, three independent experiments using human PBL exposed to laser-driven electrons and X rays (reference dose) were performed during separated beam times. Both donors were volunteers and both gave written informed consent for collection of a small amount of blood for use in the *in vitro* experiments.

### Ovarian Cancer Cells Culture and Experimental Design

The human cancer cell line OVCAR-3 was obtained from the American Type Culture Collection (Manassas, VA). Cells were cultured in RPMI 1640 media (Life Technologies, Grand Island, NY) supplemented with 20% fetal bovine serum (Sigma-Aldrich®, Munich, Germany), 100 U/ml penicillin/streptomycin (Invitrogen™, Carlsbad, CA) and 0.01 mg/ml bovine insulin (Sigma-Aldrich) at 37°C and 5% CO<sub>2</sub>. Exponentially growing cells were seeded three days before irradiation in a T25 flask at the density of  $0.7 \times 10^6$  cells/cm<sup>2</sup>. One day before irradiation, the cell culture media was completely replaced. By seeding cells in one side of the flask, an area of  $5 \times 5$  cm<sup>2</sup> is covered by the cell monolayer and positioned in the horizontal electron beam. Immediately before irradiation, the cell samples were completely filled up with culture media and finally closed with sterile Parafilm®. Cells were irradiated at 2, 4, 6, 8 and 10 Gy. Experiments were repeated three times during separated beam times to demonstrate reproducibility. Nonirradiated cell samples were prepared under the same conditions as irradiated cells and were used as controls. Immediately after irradiation cells were harvested from the 25 cm<sup>2</sup> culture flasks by trypsinization and plated at a density of  $1.8 \times 10^5$ ,  $1.2 \times 10^5$  and  $0.8 \times 10^5$  cells per well in three 6-well plates and cultured at 37°C and 5% CO<sub>2</sub> for 3, 5 and 7 days, respectively.

### Laser-Accelerated Electron Irradiations

Irradiations were performed at the Intense Laser Irradiation Laboratory (ILIL) of the National Institute of Optics of the CNR (Pisa, Italy). Blood samples and OVCAR-3 cells were irradiated at 37°C. Nonirradiated cell samples were kept under the same conditions as irradiated samples and were used as controls. DNA was extracted within 72 h for subsequent leukocyte telomere length (LTL) analysis. The electron bunches were produced by focusing the ILIL 10-TW Ti:sapphire laser pulse into a N gas-jet target at an intensity of up to  $8 \times 10^{18}$  W/cm<sup>2</sup>. The setup used for irradiation of the biological samples is shown in Fig. 1. The laser-gas interaction and acceleration regimens

were optimized by changing the laser focal spot longitudinal position inside the gas-jet and the gas-backing pressure. A rather stable regimen (exhibiting shot-to-shot fluctuations of the electron spectral features and bunch charge limited to less than 10%) was found at a backing pressure of 40 bar. Before samples were irradiated, a full dosimetric characterization of the electron source was performed. In particular, the electron spectrum and the bunch divergence were measured using a magnetic spectrometer and a SHEEBA-like detector (18). Furthermore, the dose delivered to the biological samples was retrieved by comparing experimental measurements, performed using stacks of both Gafchromic™ films (type EBT3) and sheets of water-equivalent RW3 material (PTW, Freiburg, Germany), to Monte Carlo simulations (19). It is worth noting that the use of conventional dosimeters for the characterization of laser-generated electron bunches continues to be the subject of ongoing studies, due to the ultrashort duration and ultrahigh instantaneous dose rates potentially affecting the fundamental processes underlying the detection mechanism in possible unknown ways (20). In view of these considerations, the use of Gafchromic films is, in fact, among the safest choices in the context of radiobiology experiments with laser-generated bunches. For the current studies, electron bunches with an exponential spectrum with average energy of 1.5 MeV were employed. The electron bunch divergence was measured at approximately 20° FWHM. The biological samples were placed at a distance of approximately 15 cm from the electron source. The shot-to-shot fluctuations of the bunch charge were monitored using an integrating current transformer (Fig. 1). The estimated dose per laser shot on the samples was 60 mGy. As is known, an ultrashort electron bunch is gradually stretched in time, due for instance to such phenomena as space-charge and/or energy-dispersion effects. In our case, the bunch duration at the biological sample position was estimated to be affected mostly by the scattering that occurred inside the vacuum-air window (mylar, 50 mm thick). Using Monte Carlo simulations based on the GEANT4 code (which can provide time-of-flight tracking of each particle), this bunch duration retrieved was of a few hundreds of femtoseconds. With this value, an instantaneous dose rate of around  $10^{11}$ – $10^{12}$  Gy/s can be estimated on the samples, which is well beyond the dose rate of conventional LINACs. Cumulative doses of up to 2 Gy were delivered by summing up more laser shots at a repetition rate of 0.5 Hz. To monitor the effective dose delivered to each sample, suitable stacks of Gafchromic films were placed both upstream and downstream of each sample dish. The error on the dose values measured in this way (due to issues such as the individual Gafchromic film response calibration, optical readout and comparison with Monte Carlo simulations) was estimated to be of  $\pm 5\%$ .

#### X-Ray Irradiations

To compare the biological effectiveness of laser-accelerated electrons with a reference radiation source, whole blood cells were irradiated with absorbed doses in the same range of 0–2 Gy with 50 kV X rays at a dose rate of  $94 \text{ Gy} \pm 0.4 \text{ mGy/min}$  using a conventional nonpulsed X-ray tube (Apogee; Oxford Instruments, Abingdon, UK). Dosimetric characterization of this setup was performed using thermoluminescent dosimeters as previously reported elsewhere (21). All X-ray irradiation were performed using the same tubes that were used for the laser-driven electron accelerator irradiation at the same temperature.

#### Intraoperative Radiation Therapy

A comparison of the biological effectiveness was also performed with respect to conventional, LINAC-accelerated electron beams. The NOVAC7 machine, routinely used for intraoperative radiation therapy treatments at the S. Chiara Hospital of Azienda Ospedaliero-Universitaria (Pisa, Italy), was used. In the operation mode used for this study, the machine delivered 7 MeV electron beams with a 4- $\mu$ s bunch duration at a 5 Hz repetition rate. The delivered dose was 13

cGy/pulse. A full dosimetric characterization of the machine used has been previously reported by Righi *et al.* (22).

#### Micronucleus Assay

After irradiation, 0.3 ml whole blood was mixed with 4.7 RPMI 1640 media, and the cultures were incubated at 37°C for 72 h. Cytochalasin B (6  $\mu$ g/ml) was added 44 h after culture initiation. Cells were then harvested and fixed according to standard methods (14, 15). For each sample, 1,000 binucleated cells were scored under optical microscope (final magnification 400 $\times$ ) for micronucleus analysis, following the criteria for micronucleus acceptance (14, 15). We evaluated the MN frequency as the number of micronucleated cells per 1,000 cells (‰).

#### Leukocyte Telomere Length Analysis

Leukocyte telomere length was measured quantitatively in genomic DNA using the quantitative real-time method, which measures the relative LTL by determining the ratio of telomere repeat copy number (T) to single copy gene (SG) copy number (T/S ratio) in experimental samples relative to a reference sample (23). Genomic DNA was isolated from peripheral blood leukocytes using the QIAGEN BioRobot® EZ1 System. Forward and reverse primer sequences for telomere and  $\beta$ -globin gene (SG), PCR mix and thermal cycling profile have been previously described (23). All PCRs were performed in triplicate on a 384-well CFX RT-PCR System (Bio-Rad Laboratories Inc., Hercules, CA). Samples used to construct a standard curve for telomere and SG DNAs in combination were included in each assay to evaluate amplification efficiency and linearity. Relative telomere length was calculated from:  $T/S \text{ ratio} = 2^{-\Delta Ct}$ , where  $\Delta Ct = Ct_{\text{telomere}} - Ct_{\text{SG}}$ .

#### Cell Viability Exclusion Assay

The number of viable cells was assessed by the trypan blue (Sigma-Aldrich) exclusion assay, according to the manufacturer's protocols. Briefly, after each incubation period, cells were harvested and an aliquot of 100  $\mu$ l cell suspension was incubated for 3 min at room temperature with an equal volume of 0.4% trypan blue solution that was prepared in buffered isotonic salt solution (Sigma-Aldrich). Cells were counted using a Burkert camera and viable and nonviable cells were recorded. The number of unstained (alive) cells as well as blue-colored (dead) cells were counted in 6 randomly selected fields at high magnification (40 $\times$ ). Finally, the viable cell ratio was calculated based on the following formula: viable cell ratio (%) = (unstained cell number/total cells number)  $\times$  100.

#### Statistical Analysis

All experiments were repeated at least three times. The results were expressed as mean  $\pm$  SE. Two-group comparisons were performed by the unpaired Student's *t* test. Multiple comparisons were performed by one-way analysis of variance (ANOVA) followed by a multiple comparison test (Bonferroni test). Regression analysis was used to fit all data to a linear-quadratic as well as linear model. Values of  $P < 0.05$  were considered statistically significant.

## RESULTS

#### Effectiveness of the Laser-Accelerated Electrons on Micronucleus Frequency and LTL

The dose-response curves for micronuclei yield in PBLs for each donor after irradiation with  $\sim 1.5$  MeV electrons and 50 kV X rays are shown in Fig. 2. The MN results obtained for the first donor were comparable with those of the second one. There was an increase of MN frequency

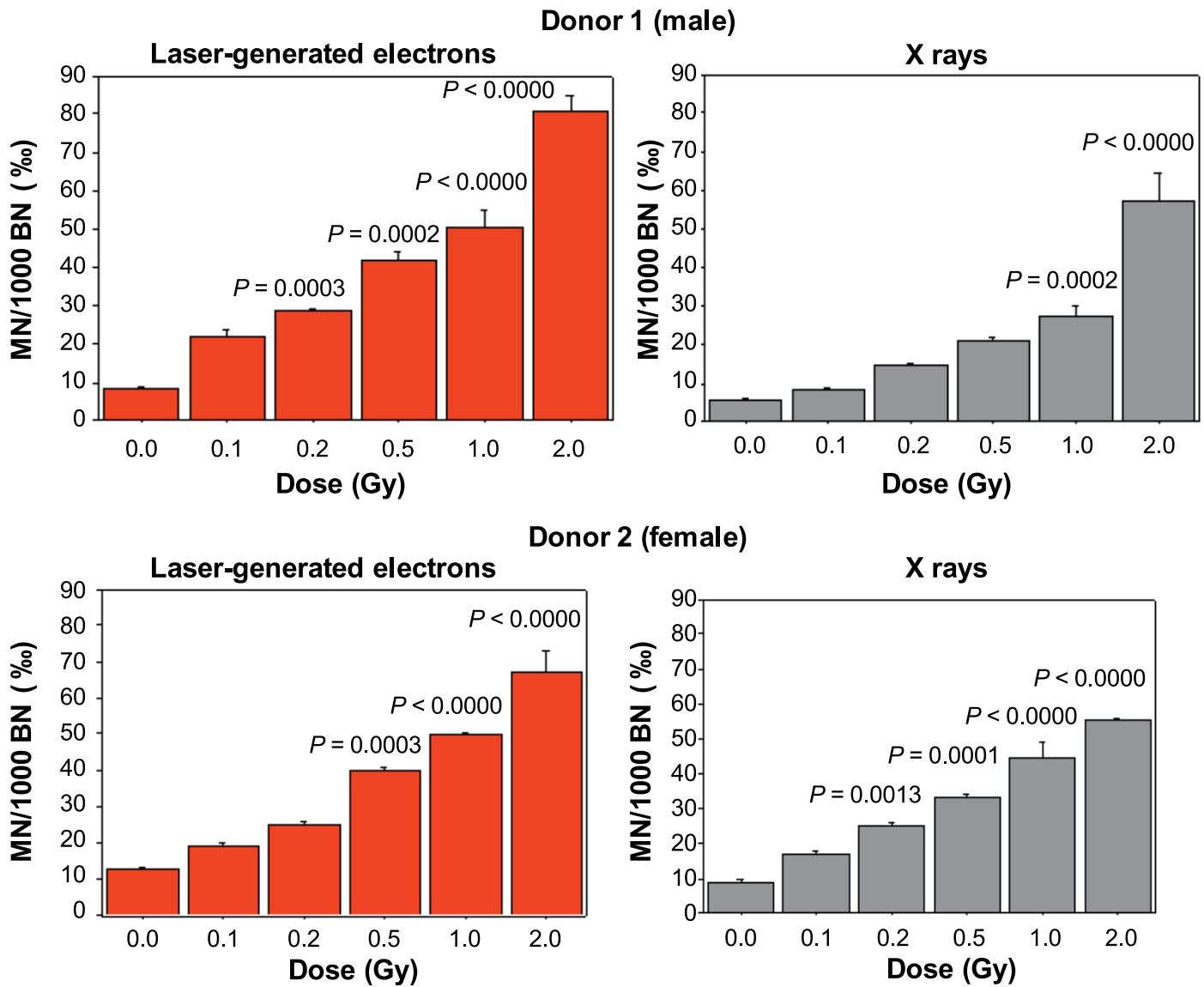


**FIG. 2.** Micronuclei per 1,000 binucleated (BN) cells in normal human PBLs as a function of doses of laser-generated electrons and X rays. All values are expressed as mean  $\pm$  SD of three independent experiments. Statistical differences were assessed for each dose compared to negative control.

with dose. Specifically, MN frequency rates were significantly higher than baseline from 0.2 ( $P = 0.0003$ ) and 0.5 Gy ( $P = 0.0002$ ) irradiation for the first and second donors, respectively. The resulting dose dependence for the effect  $Y$  was fitted to the data with the linear dose-response model ( $Y = c + \alpha D$ ), where  $Y$  is the frequency of micronuclei corresponding to a radiation dose,  $D$  Gy,  $c$  is the background MN frequency and the coefficient alpha represents the slope of the linear dose-response curve. To compare the effectiveness of the electron beam with X rays, the RBE was also evaluated. RBE is the ratio of doses that achieve the same biological effect for two radiation types. The RBE values for micronucleus induction were calculated from the alpha coefficients of the dose-response curves for electrons relative to X rays ( $RBE = \alpha_{\text{laser}}/\alpha_{\text{X rays}}$ ). The

resulting linear alpha coefficients and RBE are shown in Table 1.

Mean telomere length was found to be reduced in a significant dose-dependent manner after irradiation with both electrons and X rays (Fig. 3). There was a statistically significant difference in shortening of telomere length among the laser- and X-ray-irradiated cells (Fig. 4).

*Effectiveness of the Laser-Accelerated Electrons on Cell Survival*

Cell viability assay revealed that 6 and 8 Gy irradiation inhibited the growth of ovarian cancer cells at 5 and 7 days after laser-driven electron pulse exposures. Similarly, a 10 Gy dose inhibited the growth and proliferation of cancer

**TABLE 1**  
**Coefficients (+SEM) of Data Fitted to  $Y = c + \alpha D$  Linear Dose-Response Model for MN Induction (MN/1,000%) after Laser and X-Ray Irradiations for Two Donor Samples**

$Y = c + \alpha D$	$c$	$\alpha$	$r$	RBE = alpha laser/ alpha X rays
Donor 1				
Laser	18 ± 3.5	32.3 ± 3.8	0.974	1.3
X rays	7 ± 1.6	24.4 ± 1.7	0.990	
Donor 2				
Laser	19 ± 3.4	26.1 ± 3.6	0.964	1.2
X rays	17 ± 3.6	21.5 ± 3.8	0.941	

cells at day 3, 5 and 7 postirradiation. No significant difference was observed at 2 and 4 Gy doses (Fig. 5A).

In the case of the conventional radiofrequency accelerator for intraoperative radiotherapy, 8 and 10 Gy doses significantly inhibited cell growth on OVACR-3 cells after 5 and

7 days of incubation (Fig. 5B). Conversely, no significant response was detected at radiation doses lower than 8 Gy.

Although no statistically significant differences were observed, the OVCAR-3 cell line showed a trend toward decreased viability after exposure to the laser-driven

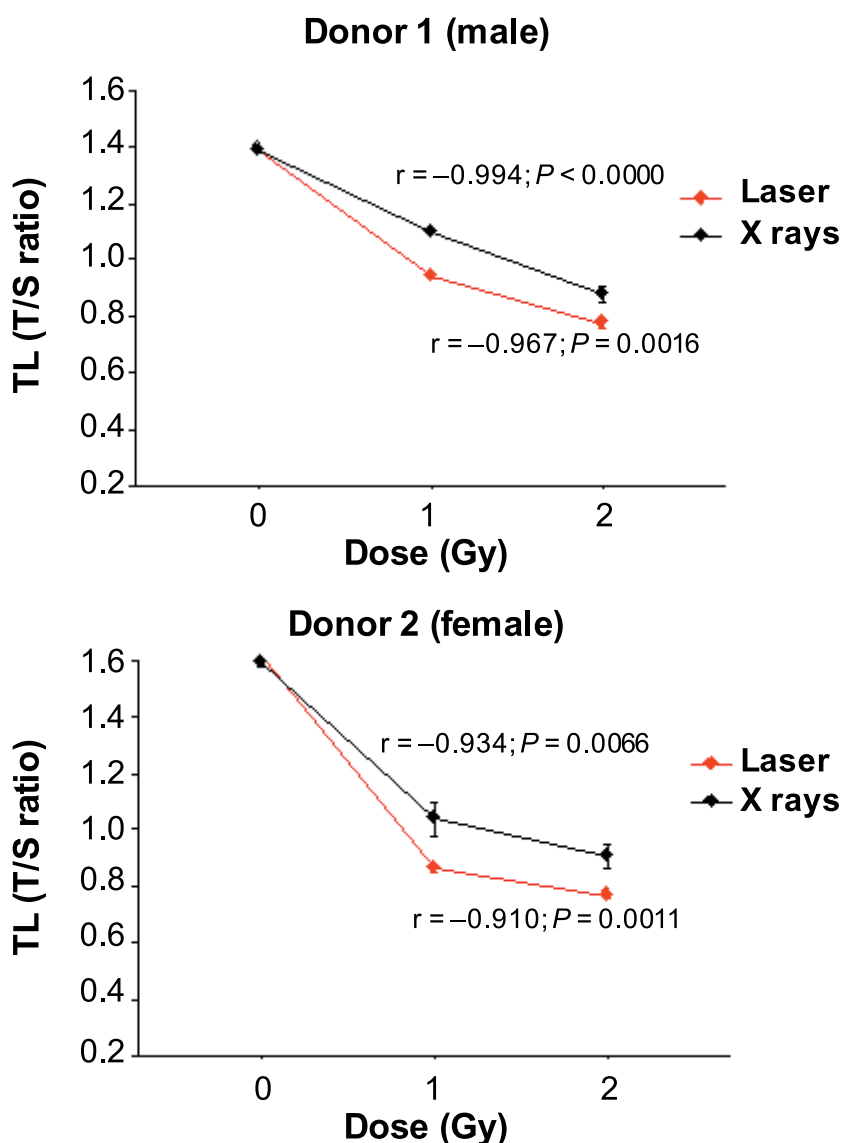


**FIG. 3.** Dose-response curve of telomere shortening in human PBLs *in vitro* irradiated with laser-generated electrons and X rays. All values are expressed as mean ± SD of three independent experiments. Statistical differences were assessed for each dose compared to negative control.

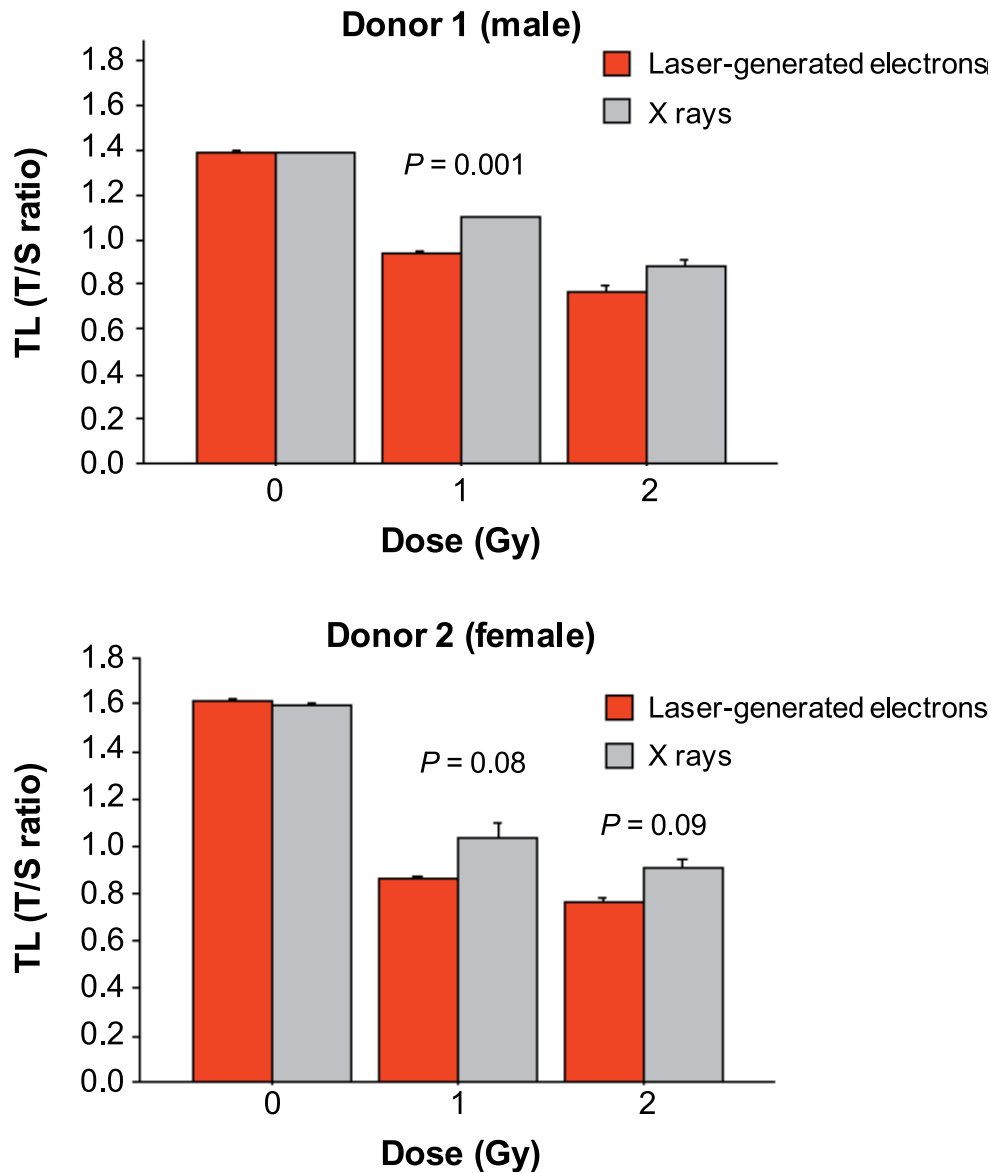


**FIG. 4.** Telomere length distributions in PBLs after irradiation with laser-generated electrons and X rays. All values are expressed as mean  $\pm$  SD of three independent experiments. Statistical differences were assessed for each dose compared to negative control.

electron pulses compared to the conventional intraoperative radiotherapy dedicated electron accelerator (Fig. 6).

## DISCUSSION

In this study, laser-driven electron pulses were found to be more effective in inducing micronuclei and telomere shortening in human PBLs compared to 50 kV X rays. Indeed, the results indicated that the MN frequency in PBLs induced by electron radiation were higher when an individual dose was compared with that of X rays. Similarly, electrons appeared more effective in inducing telomere shortening in PBLs. Moreover, findings from our *in vitro* cell experiments showed a decreased cell survival achieved by laser-accelerated pulse irradiation, suggesting a

radiobiological response similar or even higher than those measured with the conventional clinical electron beams. However, as trypan blue has been reported to underestimate X-ray induced clonogenic death in human cancer cells, our reported differences in high-energy electron versus X-ray induced cell killing may actually be greater than reported here. Further investigations will be required to test this possibility (24, 25).

Our knowledge of DNA damage in cells after electron irradiation delivered by a laser-plasma accelerator is still very limited (12, 13). Compared to conventionally accelerated particle beams, the laser-driven beams are characterized by ultrashort ( $\sim$ ps) particle pulse (bunches) duration with an ultrahigh instantaneous dose rate ( $\sim 10^{12}$  Gy  $\text{min}^{-1}$ ).

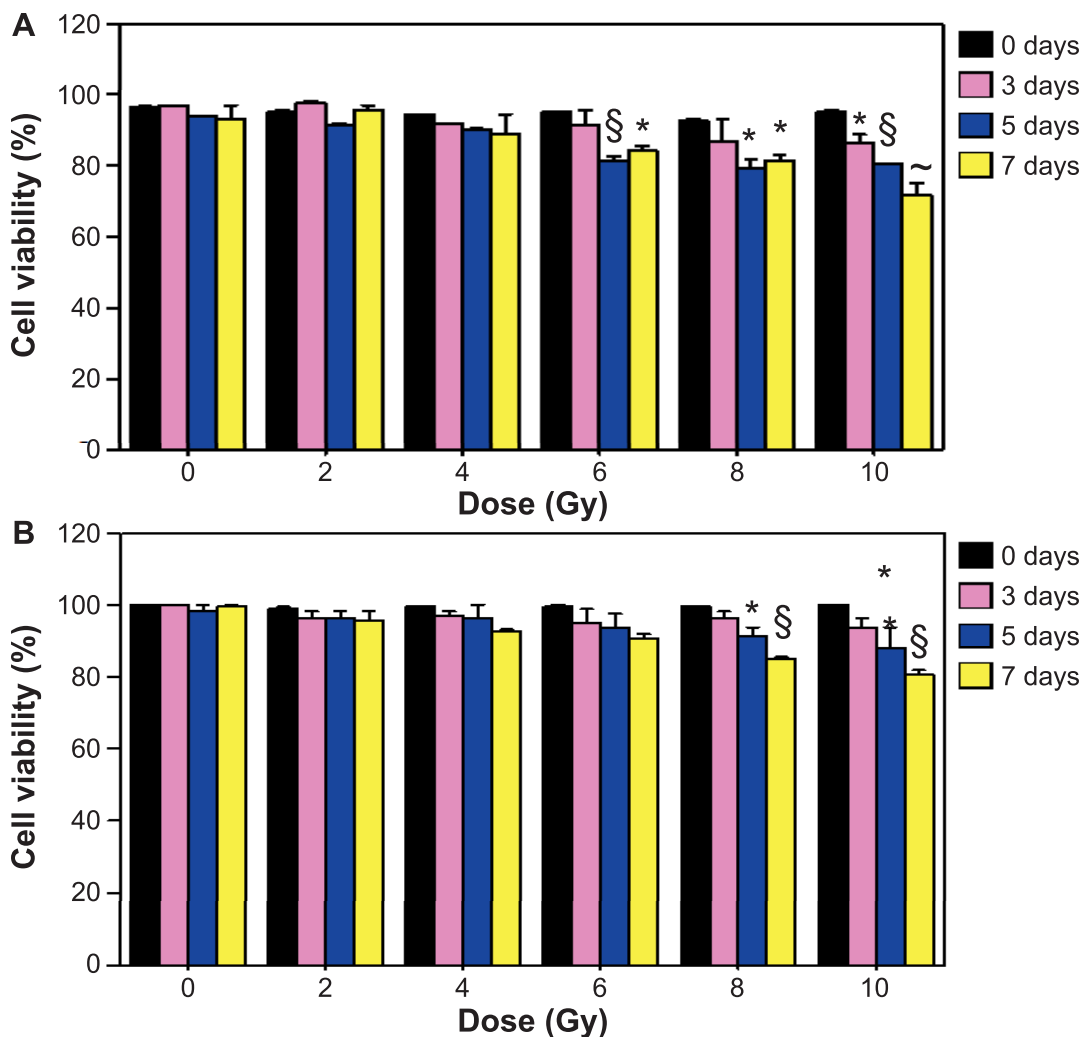


**FIG. 5.** Cell viability assay in a human cancer cell line after exposure to laser-generated electrons (panel A) and conventional accelerated particle beams (panel B). All values are expressed as mean  $\pm$  SD of three independent experiments. Statistical differences were assessed for each dose compared to negative control (\* $P \leq 0.05$ ; § $P \leq 0.01$ ; ~ $P \leq 0.001$ ).

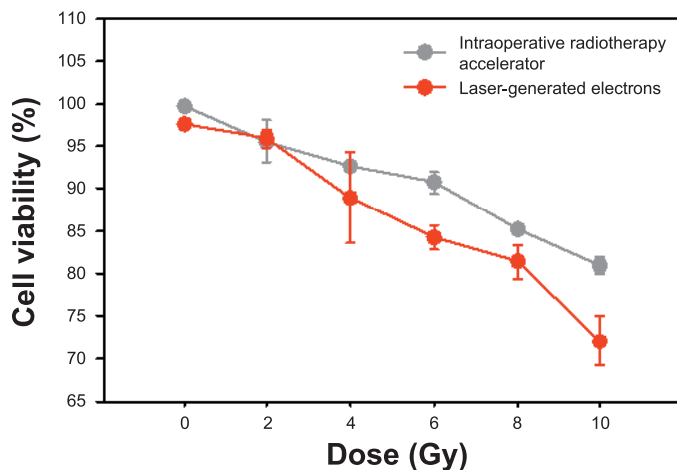


**FIG. 6.** Cell viability of OVCAR-3 at 7 days after irradiation with laser-generated electrons and conventional intraoperative radiotherapy-dedicated electron accelerator. Each point is the mean of three independent experiments; bars represent the SD ( $P = 0.07$  at 6 Gy).

The biological effectiveness of ionizing radiation is dependent on the spatial pattern of the energy deposition in nanometer volumes, particularly in DNA. DNA damage results from either a direct deposition of energy or indirectly via the action of free radicals. Among the various DNA lesions, DSBs are known to be the principal lesion. If DSBs are unrepaired or misrepaired, gene mutations, chromosomal aberrations or cell death can occur (26).

The temporal sequence of events that occurs in biological systems in response to radiation includes primary radiochemical events (radical reactions), multiple biomolecular damage (membrane and DNA lesions) and repair (12, 13). It is well understood that the physical steps leading to energy deposition occur within  $10^{-18}$  s to  $10^{-12}$  s; at the end of the physical phase, the chemical phase begins. During this latter phase, from  $10^{-13}$ – $10^2$  s, chemical radicals are formed and diffusion takes place (12). Therefore, in the case

of a laser-induced ionizing radiation pulse in the range of tens of femtoseconds, it is possible that the events of energy deposition and events of temporal sequence may modify the physical–chemical reactions within the cell.

For instance, if exposure time is very short, the biological repair events, possibly affecting the MN yields, are very remote (26). On the other hand, the energy deposition during multiple pulsed irradiations may reduce radical–radical interactions and favor more radical–DNA target interactions, thus leading to higher MN frequencies (27).

Indeed, a recent study showed that the single and multiple pulses of 7 MV electrons with varying dose rates per pulse can have a substantial effect on the MN frequency in human lymphocytes (27). However, other previous studies of X rays or electrons using nanosecond or picosecond pulsed irradiations in various mammalian cells and radiosensitive mutants showed no significant difference in radiobiological effects compared with a delivery at a conventional dose rate (28–30).

Recently, proof-of-principle experiments with laser-driven protons or electrons have also been published and in agreement with our data, these studies showed that these beams are able to generate DNA damage breaks (31–33). Finally, several groups have recently reported on *in vitro* studies evaluating the radiobiological effectiveness of laser accelerated electrons (34) and protons (35–38) relative to conventional accelerated particle beams. Altogether, these studies have shown no significant differences in the radiobiological response of laser-driven particle beams compared to conventional accelerated particle beams (34–37).

In conclusion, with rapidly evolving laser technology, specialized groups are exploring the biological effects of laser-driven particle beams. In particular, it has been found that the radiation dose deposited by very-high-energy electron beams in deep tissue is higher. This could be of potential clinical benefit for targeting deep tumors, as well as improving dose distribution and minimizing the dose burden in healthy tissue (4–6). However, the biological characteristics of laser-accelerated electrons need to be determined and compared to those of established treatment protocol before any medical applications can be considered. Our data show a radiobiological response, reflected by the induction of MN and shortening of telomere in PBLs, as well as by the reduction in survival of cancer cells after irradiation *in vitro* with laser-generated electrons.

These experiments serve as a benchmark for improving preclinical validation of radiobiological characteristics and efficacy of laser-driven electron accelerators in the future.

#### ACKNOWLEDGMENTS

Laser radiation experiments were performed at the Intense Laser Irradiation Laboratory of the INO-CNR Section in Pisa, Italy. The work of the INO-CNR Pisa group was partially supported by the Italian Ministry of Health (project no. GR-2009-1608935: Study of Radiobiological and Radiotherapeutic Effects of a Novel Laser-Driven Electron Accelerator,

D.I. AgeNaS), from the CNR-funded Italian Research Network ELI-Italy (Attoseconds) and from the PRIN project (contract no. PRIN2012AY5LEL). The Pisa authors also acknowledge contributions by the MIUR-FIRB project SPARX (Sorgente Pulsata Auto-Amplificata di Radiazione X) and the INFN Plasma-Med collaboration. We thank Dr. Fabio Di Martino, U.O. Health Physics, Azienda Ospedaliero-Universitaria Pisana (Pisa, Italy) for use of the intraoperative radiation therapy facility.

Received: September 14, 2015; accepted: April 8, 2016; published online: July 19, 2016

#### REFERENCES

1. Faure J, Glinec Y, Pukhov A, Kiselev S, Gordienko S, Lefebvre E, et al. A laser-plasma accelerator producing monoenergetic electron beams. *Nature* 2004; 431:541–4.
2. Geddes CGR, Toth C, van Tilborg J, Esarey E, Schroeder CB, Bruhwiler D, et al. High-quality electron beams from a laser wakefield accelerator using plasma-channel. *Nature* 2004; 431:538–41.
3. Mangles SPD, Murphy CD, Najmudin Z, Thomas AGR, Collier JL, Dangor AE, et al. Monoenergetic beams of relativistic electrons from intense laser-plasma interactions. *Nature* 2004; 431:535–8.
4. Malka V, Faure J, Glinec Y, Lifschitz AF. Laser-plasma accelerators: a new tool for science and for society. *Plasma Phys Control Fusion* 2005; 47:B481.
5. Malka V, Faure J, Glinec Y, Lifschitz AF. Laser-plasma accelerator: status and perspectives. *Philos Trans A Math Phys Eng Sci* 2006; 364:601–10.
6. Hooker SM. Developments in laser-driven plasma accelerators. *Nat Photonics* 2013; 7:P775–82.
7. Giulietti A, Bourgeois N, Ceccotti T, Davoine X, D'Oliveira P, Galimberti M, et al. Intense gamma-ray source in the giant dipole resonance range driven by 10-TW laser pulse. *Phys Rev Lett* 2008; 101:105002.
8. Giulietti D, Galimberti M, Giulietti A, Gizzi LA, Tomassini P, Borghesi M, et al. Production of ultra-collimated bunches of multi-MeV electrons by 35 fs laser pulses propagating in exploding-foil plasmas. *Phys Plasmas* 2002; 9:3655.
9. Gizzi LA, Benedetti C, Cecchetti CA, Di Pirro G, Gamucci G, Gatti G, et al. Laser-plasma acceleration with FLAME and ILIL ultraintense lasers. *Appl Sci* 2013; 3:559.
10. Labate L, Andreassi MG, Baffigi F, Basta G, Bizzarri R, Borghini A, et al. Small-scale laser based electron accelerators for biology and medicine: a comparative study of the biological effectiveness. *Proc SPIE* 2013; 8779. (<http://bit.ly/1XVj5jn>)
11. van Tilborg J, Schroeder CB, Filip CV, Toth CS, Geddes CGR, Fubiani G, et al. Temporal characterization of femtosecond laser-plasma accelerated electron bunches using THz radiation. *Phys Rev Lett* 2006; 96:014801.
12. Khaless AA, Karsch L, Enghardt W. Considerations on the biological effect of laser induced radiation with high dose rates. *IEEE Nucl Sci Symp Conf Rec* 2008; 3:155.
13. Malka V, Faure J, Gauduel YA. Ultra-short electron beams based spatio-temporal radiation biology and radiotherapy. *Mutat Res* 2010; 704:142–51.
14. Fenech M, Morley AA. Cytokinesis block micronucleus method in human lymphocytes; effect of *in vivo* ageing and low dose X-irradiation. *Mutat Res* 1986; 161:193–8.
15. Fenech M. The *in vitro* micronucleus technique. *Mutat Res* 2000; 455:81–95.
16. Scott D, Lyons CY. Homogeneous sensitivity of human peripheral blood lymphocytes to radiation-induced chromosome damage. *Nature* 1979; 278:756–8.
17. Sgura A, Antocchia A, Berardinelli F, Cherubini R, Gerardi S, Zilio



- C, et al. Telomere length in mammalian cells exposed to low- and high-LET radiations. *Radiat Prot Dosimetry* 2006; 122:176–9.
18. Galimberti M, Giulietti A, Giulietti D, Gizzi LA. SHEEBA: A spatial high energy electron beam analyzer. *Rev Sci Instrum* 2005; 76:053303.
  19. Lamia D, Russo G, Casarino C, Gagliano L, Candiano GC, Labate L, et al. Monte Carlo application based on GEANT4 toolkit to simulate a laser-plasma electron beam line for radiobiological studies. *Nucl Instrum Methods Phys Res A* 2015; 786:113–9.
  20. Labate L, Lamia D, Russo G. Dosimetry of laser-driven electron beams for radiobiology and medicine. In: Giulietti A, editor. *Laser-driven particle acceleration towards radiobiology and medicine*. Berlin Heidelberg: Springer-Verlag; 2016.
  21. Cervelli T, Panetta D, Navarra T, Andreassi MG, Basta G, Galli A, et al. Effects of single and fractionated low-dose irradiation on vascular endothelial cells. *Atherosclerosis* 2014; 23:510–8.
  22. Righi S, Karaj E, Felici G, Di Martino F. Dosimetric characteristics of electron beams produced by two mobile accelerators, Novac7 and Liac, for intraoperative radiation therapy through Monte Carlo simulation. *J Appl Clin Med Phys* 2013; 14:6–18.
  23. Sabatino L, Botto N, Borghini A, Turchi S, Andreassi MG. Development of a new multiplex quantitative real-time PCR assay for the detection of the mtDNA 4977 deletion in coronary artery disease patients: a link with telomere shortening. *Environ Mol Mutagen* 2013; 54:299–307.
  24. Carmichael J, DeGraff WG, Gazdar AF, Minna JD, Mitchell JB. Evaluation of a tetrazolium-based semiautomated colorimetric assay: assessment of radiosensitivity. *Cancer Res* 1987; 47:943–6.
  25. Citrin, DE. Short-Term Screening Assays for the Identification of Therapeutics for Cancer. *Cancer Res* 2016; 76:3443–5.
  26. Hall EJ, Brenner DJ. The dose-rate effect revisited: radiobiological considerations of importance in radiotherapy. *Int Radiat Oncol Biol Phys* 1991; 21:1403–14.
  27. Acharya S, Bhat NN, Joseph P, Sanjeev G, Sreedevi B, Narayana Y. Dose rate effect on micronuclei induction in human blood lymphocytes exposed to single pulse and multiple pulses of electrons. *Radiat Environ Biophys* 2011; 50:253–63.
  28. Tillmann C, Grafstrom G, Jonsson AC, Jonsson BA, Mercer I, Mattsson S, et al. Survival of mammalian cells exposed to ultrahigh dose rates from a laser-produced plasma X-ray source. *Radiology* 1999; 213:860–5.
  29. Shinohara K, Nakano H, Tago M, Kodama R. Effects of single-pulses ( $\leq$  or  $=$  1 ps) X-rays from laser-produced plasmas on mammalian cells. *J Radiat Res* 2004; 45:509–14.
  30. Sato K, Nishikino M, Okano Y, Ohshima S, Hasegawa N, Ishino M, et al. Gamma-H2AX and phosphorylated ATM focus formation in cancer cells after laser plasma X irradiation. *Radiat Res* 2010; 174:436–45.
  31. Yogo A, Sato K, Nishikino M, Mori M, Teshima T, Numasaki H, et al. Application of laser-accelerated protons to the demonstration of DNA double-strand breaks in human cancer cells. *Appl Phys Lett* 2009; 94:181502.
  32. Kraft SD, Richter C, Zeil K, Baumann M, Beyreuther E, Bock S, et al. Dose-dependent biological damage of tumour cells by laser-accelerated proton beams focus on laser- and beam-driven plasma accelerators. *New J Phys* 2010; 12:085003.
  33. Rigaud O, Fortunel NO, Vaigot P, Cadio E, Martin MT, Lundh O, et al. Exploring ultrashort high-energy electron-induced damage in human carcinoma cells. *Cell Death Dis* 2010; 1:e73.
  34. Laschinsky L, Baumann M, Beyreuther E, Enghardt W, Kaluza M, Karsch L, et al. Radiobiological effectiveness of laser accelerated electrons in comparison to electron beams from a conventional linear accelerator. *J Radiat Res* 2012; 53:395–403.
  35. Yogo A, Maeda T, Hori T, Sakaki H, Ogura K, Nishiuchi M, et al. Measurement of relative biological effectiveness of protons in human cancer cells using a laser-driven quasimonoenergetic proton beamline. *Appl Phys Lett* 2011; 98:053701.
  36. Doria D, Kakolee KF, Kar S, Litt SK, Fiorini F, Ahmed H, et al. Biological effectiveness on live cells of laser driven protons at dose rates exceeding 109 Gy/s. *AIP Adv* 2012; 2:011209.
  37. Bin J, Allinger K, Assmann W, Dollinger G, Drexler AG, Friedl AA, et al. A laser-driven nanosecond proton source for radiobiological studies. *Appl Phys Lett* 2012; 101:243701.
  38. Zeil K, Baumann M, Beyreuther E, Burris-Mog T, Cowan TE, Enghardt W, et al. Dose controlled irradiation of cancer cells with laser accelerated proton pulses. *Appl Phys B* 2013; 110:437–44.